

POINT SPREAD FUNCTION OF A PASSIVE VISION SYSTEM FOR THE CASE OF SMOKE AEROSOL

B.D. Borisov

*Institute of Atmospheric Optics,
Siberian Branch of the Russian Academy of Sciences, Tomsk
Received December 27, 1995*

The technique and results are considered of the experiment on measuring the point spread function (PSF) of a passive system for vision through smoke aerosol generated in the limited space of a large volume with the optical thickness $\tau = 0.16$ to 2.94. The qualitative comparison is carried out with the PSF of vision systems under conditions of winter atmospheric hazes and wood smoke.

Only little information about the experimental results on the image transfer in the scattering atmosphere and the relations of the image characteristics with the aerosol microstructure parameters is available in the literature.¹ It is first of all connected with the certain technical and financial difficulties in arranging such experiments in real atmosphere, for example, such as to measure the fundamental characteristic of a passive vision system, the point spread function (PSF).

For these reasons, it is expedient to measure PSF in the media modeling the most characteristic states of the aerosol atmosphere. The haze^{2,3} is one of such frequently observed states of turbid atmosphere in the majority of geographical regions.

The comparison of the optical characteristics of atmospheric hazes with corresponding optical characteristics of the smoke aerosols showed that the principal peculiarities of the shape of the scattering phase function and the degree of polarization, as well as the limits of the variability of smokes in the visible wavelength range, are very similar to the atmospheric hazes.³ The study of the image transfer in smokes has its own significance, in particular, for the development of the vision systems operating in smokes when fighting fires and for other extremal events. The interest in studying the smoke aerosol has noticeably increased in recent decade due to its possible effect on the ecological situation and climate change.⁴⁻⁷

The principal characteristics of the smoke variability are the smoke content at the smoke generation stage, temperature of decomposition of the substance, relative humidity of air and "aging" of the smoke aerosol with time. When the continuously operating source of new smoke particles is absent, the principal variations of the extinction coefficient ϵ occur during two first hours after its formation.⁴⁻⁶

The particle size distribution of the settled wood smokes within a limited volume approaches the single-mode one with the median radius near 0.1–0.3 μm (Refs. 3 and 4).

Thus, the information available allows one to compose the broad outlines of the properties of wood smoke aerosol, that allowed us to manage without additional investigations when measuring and analyzing PSF, the results of which are presented in this paper.

The meaning of the point spread function $h(x - \xi, y - \eta)$ in the linear vision systems consisting of the imaging optical system, scattering medium and object plain is clear from the relationship

$$g(x, y) = \iint_{-\infty}^{+\infty} h(x - \xi, y - \eta) o(\xi, \eta) d\xi d\eta, \quad (1)$$

where $g(x, y)$ and $o(\xi, \eta)$ are the illumination distribution on the image and brightness distribution of the object, respectively; (x, y) and (ξ, η) are the coordinates of points of the image and of the object. It follows from Eq. (1) that $h(\xi, \eta)$ characterizes the contribution of the object points spaced at the distance of $0 < r = \sqrt{\xi^2 + \eta^2} < \infty$ from the object point at the axis of the vision system into the illumination observed at the point $x = 0, y = 0$, through the scattering channel. An exact direct method of determining PSF follows from Eq. (1), different from the approximate one based on determining the illumination distribution in the image of elementary Lambert source in the object plane.⁸

The experiments were carried out in the big aerosol chamber (BAC) of the volume $V = 1780 \text{ m}^3$, that allows the simulation of different aerosol formations in it (adiabatic expansion, evaporation and dispersion fogs, smog formations of the smoke type, etc.).

Direct technique or technique of spatial scanning was used for measuring PSF. The KGM-300 halogenic lamp simulated the model of the point source T . It was mounted on a special cart with a cylindrical modulator of the light flux (Fig. 1) with the modulation frequency of 150 Hz. The source with the

modulator moved along the guide H installed inside the BAC by means of the electrical drive D with the clearanceless reducer switched by the steel rope system. To control the source position (i.e. to determine its coordinates), we used a disk with slits that chopped the light flux from the lamp situated behind the disk and generated the pulsed light flux at the photodiode situated at another side of the disk. The disk was mounted on the electrical drive axis. When switching on the drive and moving the radiation source, the pulse signal from the photodiode enters the frequency measurer SI of the C3-57 type operating in the pulse counting mode. The scale value of the spatial coordinate r in the object plane corresponded to 436 pulses on the counter, when moving the source to 10 mm, that allowed us to determine r with a sufficient accuracy.

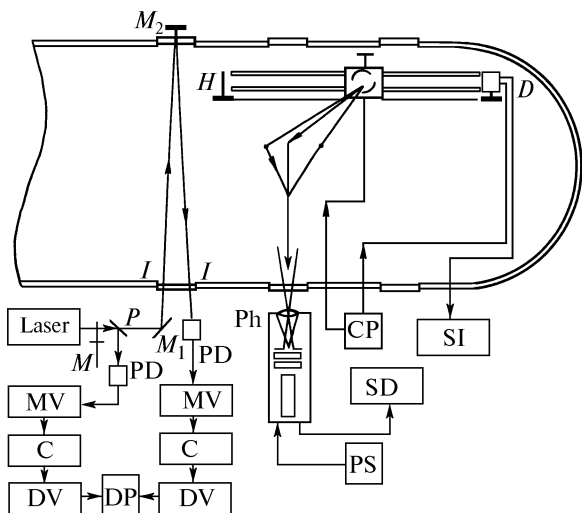


FIG. 1. Block diagram of the experimental setup.

The source could be mounted and fixed at any position on the guide by means of the remote control panel (CP). The distance between the receiving objective and the source was $L = 8.5$ m ($L = r/\tan\alpha$, where α is the angle between the optical axis and the direction to the source), if the latter had been placed on the optical axis of the receiving system.

The measuring photometer and the complex of receiving and measuring instrumentation was outside the chamber. The light flux was recorded through the chamber window equipped with the prompt opening system.

The photometer Ph included the standard set of optical-mechanical devices necessary for performing such measurements, and consisted of the I-37 objective with 300 mm focal length, field diaphragm composed from crossing controlled UF-1 slits, interference filter with the maximum transmission at $\lambda = 0.602$ μ m, changeable neutral filters and photoelectric multiplier with the power supply block (PS). The field of view

of the photometer was determined by the source image size and was $2.3 \cdot 10^{-4}$ rad. The signal from the photoelectric multiplier was recorded with a selective device (SD) of 237 type at the fixed position of the source.

Second measuring channel was used for a continuous control of the density of smoke aerosol. The beam from a laser of the LG-79 type at $\lambda = 0.63$ μ m was modulated by the electromechanical chopper M at the frequency of 1 kHz (Fig. 1). The modulated beam was directed to the scattering medium through the BAC window by means of a beam-folding mirror (M_1), then it passed through the chamber and was directed to photodetector (PD) by the mirror M_2 . Then it was amplified and recorded by a selective microvoltmeter (MV). The radiation source stability was controlled by another PD sensor, to which the radiation was directed through a semitransparent plate P .

The FD-24K photodiodes were used for converting the light flux into the electrical signal. The signals of microvoltmeters came to the digital voltmeters (DV) of the 4014A type through the converters (C) of the V9-6 type, and then to the digital printer (DP) for simultaneously recording the measured and reference signals.

When measuring the PSF in smoke aerosol, the technique was constructed taking into account the peculiarity of formation of the stable state of its microphysical characteristics. The chamber, well cleaned by blowing air, was filled with wood smoke aerosol produced by burning wood. Then the smoke aerosol was settled in the closed chamber during few hours. The cycles of measurement of PSF were carried out in the stable "aged" smoke aerosol. Then the density of smoke aerosol was decreased by pumping it out. We supposed that humidity inside BAC did not significantly change, because the measurements were carried out during the cold season, and, when pumping out, the smoke was "diluted" with air of practically the same humidity. Such a technique made it possible to measure the PSF in smoke aerosol of approximately the same microphysical characteristics. One can assume that the smoke aerosol has a single-mode distribution with the median radius of particles at 0.1 to 0.3 μ m during these measurements, and only its density changed. The time of measurement of one PSF curve was approximately half an hour, during which τ could be changed by 1.5-3.5% of its initial value.

The results of one of the measurement cycle in smoke aerosol are shown in Fig. 2. The y -axis is $h(r, \tau)$ normalized to its maximum value at different optical depths, and the x axis is the coordinate of the point source in the object plane. The curve 1 in Fig. 2 is measured when the smoke aerosol was absent, i.e. it corresponds to the instrumentation function of the vision system considered. Curves 2 to 6 ($\tau = 0.16$ to 2.94) are obtained from the measurement cycles in smoke aerosol along the path L long.

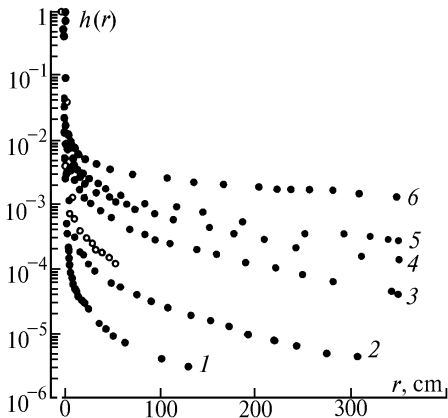


FIG. 2. PSF of the vision system as a function of τ for wood combustion smokes: 1) $\tau = 0$; 2) 0.16; 3) 1.12; 4) 1.74; 5) 2.16; 6) 2.94; \circ is for winter haze.

Analysis of the experimental results shown in Fig. 2 makes it possible to isolate three parts of the brightness profiles of PSF in smoke aerosol. The first one is in the coordinate range $r = 0$, where the relative value of brightness sharply decreases as r increases; it determines the recorded part of the direct radiation of the point object. Then there is a part of transition to a linear decrease of brightness of the scattered radiation in a semi-logarithmic coordinates with the further increase of r . Because of a PSF symmetry, one can characterize the transition part, as τ increases, by the radius R determining the beginning of the prevalent contribution of the higher orders of the scattered light into the brightness recorded. The coordinate r in the cross point of the linear part of the PSF "wing" with its transition part (Fig. 2), determined graphically from the experimental profiles of the PSF, was taken as the value R at a set τ .

The value R as function of τ is shown in Fig. 3. The increase of the optical depth leads to the quick decrease of the transition part. The graphical analysis of the curve in Fig. 3 shows that the change of R as the optical depth increases can be represented under given conditions of the experiment in the form $R = 89 \exp(-0.23\tau)$ with the mean approximation error of 4%.

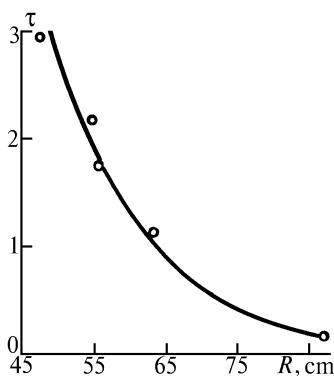


FIG. 3. Transition part radius R as a function of τ .

The relative brightness of the scattered radiation in the PSF wings also decreases with increasing spatial coordinate r according to the exponential law characteristic of the multiple scattering. This law can be violated at increased τ and higher orders of multiple scattering.⁹

It should be also noted that, according to Ref. 6, the technique for smoke generation (combustion) used in the experiments leads to generation of absorbing smoke aerosol with the single scattering albedo $\Lambda \sim 0.3-0.4$. It can cause a redistribution of the effective multiplicities of scattering due to absorption and raise the role of the low multiplicities in comparison with the smokes generated by the pyrolysis technique.² One should expect an increase in R and extension of the exponential law on r to greater τ in such smokes.

The relation to the aerosol atmosphere is illustrated by circles (Fig. 2) that show the values of normalized PSF of the vision system, experimentally obtained in the real atmosphere and averaged over several measurement series. The measurements were carried out by the author at the field area of the Institute of Atmospheric Optics under the dense haze conditions in winter nights. The technique of angular scanning was used in the measurements. The measurement path length was equal to 31.5 m. The modulated KGM-100 lamp simulated the point object. Temperature of the ambient air changed from -18 to -20°C from cycle to cycle. Disperse composition of the medium was measured with an AZ-5 photoelectric counter of aerosol particles.¹⁰

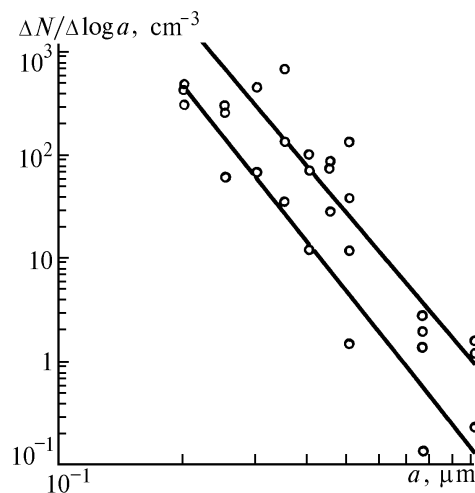


FIG. 4. Size distribution of the number density of winter haze particles.

Samples of the size distribution of winter haze aerosol particles obtained in the accompanying measurements of the PSF are shown in Fig. 4. It is seen in Fig. 4 that the aerosol particles of winter haze measured with this instrument have radii $a = 0.2$ to $0.5 \mu\text{m}$.

The results presented confirm the fact that the studies of the smoke aerosol in the limited volume can describe the pulse response of the real aerosol atmosphere with a good qualitative agreement, at least, at not very large optical depths.

REFERENCES

1. E.P. Zege, A.P. Ivanov and I.L. Katsev, *Image Transfer in Scattering Media* (Nauka i Tekhnika, Minsk, 1985), 327 pp.
2. V.E. Zuev and M.V. Kabanov, *Transfer of Optical Signals in the Earth's Atmosphere (under Interference Conditions)* (Sov. Radio, Moscow, 1977), 368 pp.
3. V.E. Zuev and V.Ya. Fadeev, *Laser Navigation Devices* (Radio i Svyaz', Moscow, 1987), 160 pp.
4. V.S. Kozlov, "Experimental investigations of optical and microphysical properties of smoke aerosols," Authors Abstract of Cand. Phys.-Math. Sci. Dissert., State University, Tomsk (1985).
5. G.S. Golitsyn, A.K. Shukurov, A.S. Ginzburg, et al., *Izv. Akad. Nauk SSSR, Ser. Fiz. Atmos. Okeana* **24**, No. 3, 227–234 (1988).
6. V.S. Kozlov, M.V. Panchenko, and A.G. Tumakov, *Atmos. Oceanic Opt.* **6**, No. 10, 735–738 (1993).
7. S.D. Andreev, L.S. Ivlev, E.F. Mikhailov, et al., *Atmos. Oceanic. Opt.* **8**, No. 5, 355–357 (1995).
8. V.V. Belov, B.D. Borisov, V.N. Genin, et al., *Izv. Akad. Nauk SSSR, Ser. Fiz. Atmos. Okeana* **23**, No. 11, 1205–1210 (1987).
9. A.P. Ivanov, *Physical Principles of Hydrooptics* (Nauka i Tekhnika, Minsk, 1975), 503 pp.
10. A.P. Klimenko, *Techniques and Instrumentation for Measuring the Dust Concentration* (Khimiya, Moscow, 1978), 207 pp.